Effect of zirconium(IV) propoxide concentration on the thermophysical properties of hybrid organic-inorganic films

Tao Wang,[1,2] Xinwei Wang,[3,a)] Yanwu Zhang,[4] Liying Liu,[4] Lei Xu,[4] Ying Liu,[4] Lijun Zhang,[2] Zhongyang Luo,[1] and Kefa Cen[1]
[1]*State Key Laboratory of Clean Energy Utilization, Zhejiang University, Hangzhou 310027, People's Republic of China*
[2]*Department of Mechanical Engineering, N104 Walter Scott Engineering Center, University of Nebraska-Lincoln, Lincoln, Nebraska 68588-0656, USA*
[3]*Department of Mechanical Engineering, 3027 H.M. Black Engineering Building, Iowa State University, Ames, Iowa 50011-2161, USA*
[4]*Department of Optical Science and Engineering, School of Information Science and Technology, Fudan University, Shanghai 200433, People's Republic of China*

(Received 4 March 2008; accepted 26 April 2008; published online 11 July 2008)

In this work, micrometer-thick organic-inorganic hybrid films are fabricated. A photothermal experiment is designed and conducted to characterize the thermophysical properties of hybrid films, as well as the thermal contact resistance between the film and substrate. The molecular cagelike or nanopores, which can strongly enhance the phonon scattering, are considered to be formed inside the films during fabrication. The first order estimation of the volume fraction of cavities and its effect on thermophysical properties are obtained. The effect of zirconium(IV) propoxide (ZPO) concentration on the thermophysical properties of hybrid films is also studied. The effective (measured) thermal conductivity and thermal effusivity of hybrid films are close to those of polymethyl methacrylate (PMMA) films, and are not significantly affected by the added ZPO, which is used to adjust the optic properties of films. The extracted bulk thermal conductivity of the hybrid films is close or smaller than that of bulk PMMA, and shows certain thermal conductivity reduction by the ZPO addition. The thermal effusivity study indicates that the response of the surface temperature change to an abrupt heat flux across the surface of hybrid films will be similar to that of PMMA films. © *2008 American Institute of Physics*. [DOI: 10.1063/1.2951961]

I. INTRODUCTION

Thermal conductivity is a fundamental property of materials. Knowledge about this property is critical for high-degree control of the heat flow through thin films in applications such as device packaging. In the field of integrated optics, many waveguide devices work based on the thermo-optic effect. The refractive index of the waveguide is temperature tuned to realize functions such as switching and modulation. For thermo-optic devices, thermal conductance is an important coefficient which has significant influence on the response time of devices. Recently, organic [polymethyl methacrylate (PMMA)]/inorganic hybrid materials attracted significant attention in applications in integrated optics. It was found that hybrid materials have excellent thermo-optic coefficient, as well as thermal and chemical stabilities.[1] We reported very low electric power consumption optical switches and variable optical attenuators based on hybrid materials.[2] However, up to now, the thermal properties of the materials are not well studied.

PMMA is an amorphous, colorless thermoplastic material of excellent optical transparency and a luminous transmittance of about 92%.[3] In the past, bulk PMMA has been successfully used as a transfer standard for thermal conductivity.[3–6] In 2004, an intercomparison of measurements of thermal conductivity, thermal diffusivity, specific heat capacity, and density of PMMA in the temperature range between −70 and +80 °C involving 17 European laboratories was conducted by Rudtsch and Hammerschmidt.[3] In this intercomparison, the thermal conductivity values produced at 30 °C ranged from 0.16 to 0.21 W/m K. It was proposed that the possible reason for this discrepancy was the not properly treated effect of contact resistance. A transient hot-wire technique has been employed by Assael *et al.*[4] to measure the thermal conductivity of bulk PMMA at a temperature ranging from room temperature up to 350 K. The thermal conductivity value varies from 0.1922 to 0.1986 W/m K. Putnam *et al.*[5] measured the thermal conductivity of bulk PMMA using the 3ω method, and attained a value of 0.205 W/m K at 280 K. The thermal conductivity of PMMA film may differ significantly from the bulk value due to the difference in microstructure such as the grain size, amorphousness, and concentration of foreign atoms and defects, which strongly affect the scattering process of energy carriers. A noncontact thermoreflectance technique was employed by Chu *et al.*[7] to measure the thermal conductivity of PMMA films (0.4 μm thick), and a smaller value of 0.16 W/m K was obtained and compared with the bulk value. In this method, the sample was spin coated on silicon substrate and a 400-nm-thick aluminum layer was deposited on top of the sample. Govorkov *et al.*[8] also measured the PMMA films spin coated on silicon substrates and values

a)Author to whom correspondence should be addressed. Electronic mail: xwang3@iastate.edu. Tel.: 515-294-2085. FAX: 515-294-3261.

about 0.14 W/m K were obtained for films with thickness from 0.1 to 0.8 μm. In their experiment, a differential photoacoustic method was developed and used.

In the last decade, many techniques have been developed to measure the thermophysical properties of thin film materials. There are two categories of techniques for thermal conductivity measurement: contact and noncontact methods. In contact measurements, normally a thin metal film is deposited onto the sample surface that is subsequently patterned into electric circuitry. The temperature response of the sample structure under thermal loading is sensed by the circuit, and related to unknown thermal properties.[9] The 3ω and extended 3ω method,[10,11] pulse heating method,[12] and microbridge method[13,14] fall in this category. Drawbacks of the contact methods are that they are limited to dielectric thin films, and the sample preparation process is laborious. In the noncontact method, optical techniques are mainly used, for which the optical response using a probing beam is measured when the sample is subjected to photothermal excitation. The thermal conductivity of the sample can be obtained by measuring the phase shift of the reflected beam due to surface deformation,[15] the reflectivity change due to pulse laser heating,[14] or deflection of the probing beam due to change of the refractive index of air near a heated sample.[16]

In this work, organic (PMMA)-inorganic (SiO_2, ZrO_2) hybrid films with different molar concentration of ZrO_2 are synthesized. A photothermal experimental technique is developed and used to characterize the thermal properties of films. The effects of structure of films on the thermal properties, such as the thermal conductivity and thermal effusivity, are analyzed. The experimental principles and details are presented in Sec. II and the experimental results are discussed in Sec. III.

II. SAMPLE PREPARATION AND CHARACTERIZATION

A. Sample preparation

The organic-inorganic hybrid materials used are synthesized using the sol-gel method, with the hydrolysis and polycondensation of methacryloxypropyl trimethoxysilane (MAPTMS), methacrylic acid (MAA), and zirconium(IV) propoxide (ZPO). The inorganic part of MAPTMS is first prehydrolyzed to form SiO_2 network with aqueous HCl catalyst. The organic part of MAPTMS is polymerized to form PMMA network under UV light exposure. ZPO is mixed with MAA to produce ZrO_2, which is used to adjust the refractive index of the product. After mixing MAPTMS and ZPO, a photoinitiator (IRGACURE 819, CIBA) is finally added into the sol. Different types of sol are prepared with different molar ratios of MAPTMS:ZPO. They are used as waveguide core and cladding/buffer materials, respectively. Thin films are formed by dip coating the sol on silicon substrate and heating it subsequently. After preheating, they are exposed to UV light for polymerization of the organic part of the hybrids. After UV exposure, another heating process is conducted for densification. Thickness of the films is measured by a profilometer (Zygo NewView 200).

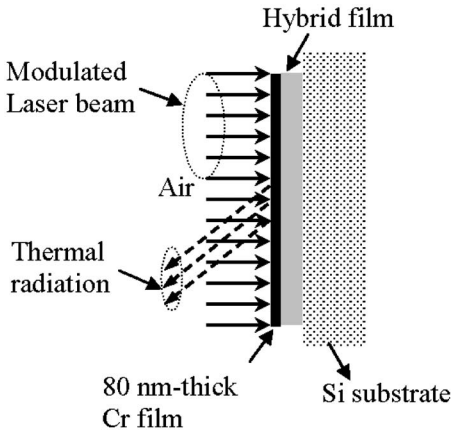

FIG. 1. Schematic of the experimental principle.

B. Thermal Characterization

1. Experimental setup and details

We use the noncontact photothermal technique to measure the out-of-plane thermal conductivity of the hybrid films. Figure 1 shows the principles of the experiment. In order to reduce the effect of moisture in the material, the samples are preheated for 1 h at 110 °C. Then an 80-nm-thick Cr film is sputtering coated (Emitech K575X) on top of the film before the measurement. A modulated laser beam is used to irradiate the surface of the Cr film. As a result, the laser beam induces direct heating of the Cr film, leading to a periodic temperature variation at the Cr surface. The heat conduction of sample film strongly affects this temperature variation, which is sensed by measuring the surface thermal radiation. The phase shift of the thermal radiation relative to the laser beam is measured and used to determine the thermophysical properties of the sample.

Figure 2 shows how the experiment is arranged and operated. A continuous infrared diode laser (BWTEK BWF-2, 809 nm wavelength) is modulated by a function generator and then is directed and focused on the sample. Different laser powers will heat the sample to different temperatures, which may affect the thermophysical properties of the samples. In our experiment, a laser beam about 600 mW (after modulation) is used, which assures sufficiently high thermal radiation signal from the Cr surface while keeping the sample temperature increase moderate to preclude large change of the thermophysical and optical properties of the

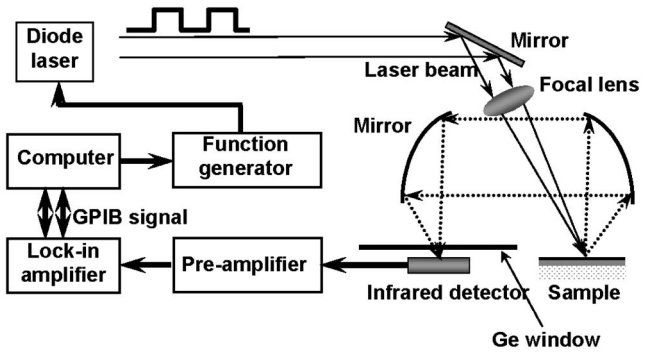

FIG. 2. Schematic of the experimental setup.

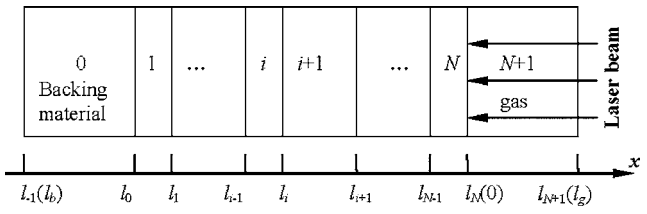

FIG. 3. Schematic of a N-layer sample (Ref. 18).

sample. The laser beam has a Gaussian distribution in space. In the experiment, the spot of the laser beam on the sample is about 0.7×1.4 mm^2 (Ref. 17) (the beam is not perpendicular to the sample surfaced), which is much larger than the thermal diffusion depth in the lateral direction of the sample. As a result, the Gaussian distribution will have negligible effect on the measured phase shift. The thermal radiation from the Cr film (refer to Fig. 1) is directed to an infrared detector. A Ge window is placed in front of the infrared detector to filter out the reflected laser beam and allows only the thermal radiation to pass. The signal from the infrared detector is preamplified and then is measured by a lock-in amplifier. The experiment is controlled by a personal computer for automatic data acquisition.

2. Physical model and data processing

The phase shift of the thermal radiation is measured over a large frequency range. In the experiment, the light source is a modulated monochromatic laser beam of wavelength λ, incident through the nonabsorbing gas (air) on the sample with flux $I=I_0(1+\cos\omega t)/2$ (here we only consider the ω component in the square wave laser beam), where ω is the modulated angular frequency of the incident light. The heating spot (the size of the focal point of the laser beam) is about 0.7×1.4 mm^2.[17] Considering the thickness of samples, the modulation frequency of the laser beam is set between 0.2 and 20 kHz. Within this frequency range, the thermal diffusion depth within one heating period in the lateral direction of the sample is much smaller than the heating spot. As a result, the thermal transport induced by laser heating can be treated one-dimensional along the thickness direction of the sample. Therefore, for a multilayer sample, as shown in Fig. 3 (cross-sectional view), the thermal diffusion equation in layer i can then be expressed as[18]

$$\frac{\partial^2\theta_i}{\partial x^2}=\frac{1}{\alpha_i}\frac{\partial\theta_i}{\partial t}-\frac{\beta_i I_0}{2k_i}\exp\left(\sum_{m=i+1}^{N}-\beta_m L_m\right)\times e^{\beta_i(x-l_i)}(1+e^{j\omega t}), \tag{1}$$

where α_i, β_i, and k_i are the thermal diffusivity, optical absorption, and thermal conductivity of layer i, respectively. $L_i=l_i-l_{i-1}$ and $\theta_i=T_i-T_{\text{amb}}$ are the thickness and modified temperature in layer i, respectively, and T_{amb} is the ambient temperature.

The solution θ_i to Eq. (1) consists of three parts: the transient component, the steady dc component, and the steady ac component. Only the ac component $\tilde{\theta}_{i,s}$ can be picked up by the lock-in amplifier, which can be expressed in the form of[18]

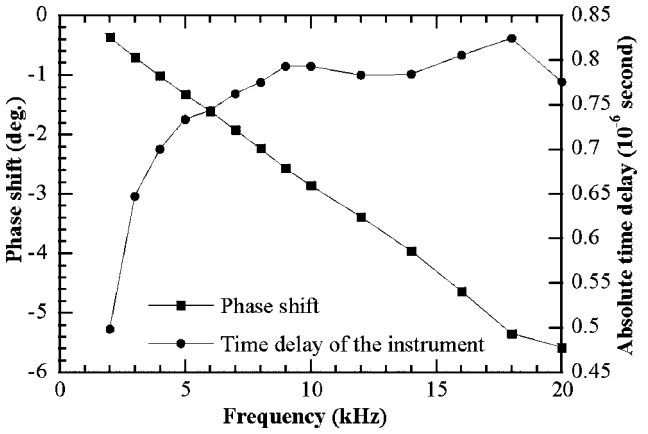

FIG. 4. Measured phase shift of the reflected laser beam and absolute time delay induced by the instrument.

$$\tilde{\theta}_{i,s}=(A_i e^{\sigma_i(x-h_i)}+B_i e^{-\sigma_i(x-h_i)}-E_i e^{\beta_i(x-h_i)})e^{j\omega t}, \tag{2}$$

where $h_i=l_i$ for $i=0,1,\ldots,N$, and $h_{N+1}=0$. σ_i is defined as $(1+j)\sqrt{\omega/2\alpha}$ with $j=\sqrt{-1}$. A_i and B_i are the coefficients to be determined which can be obtained in a matrix form as

$$\begin{bmatrix}A_i\\B_i\end{bmatrix}=U_i\begin{bmatrix}A_{i+1}\\B_{i+1}\end{bmatrix}+V_i\begin{bmatrix}E_i\\E_{i+1}\end{bmatrix}. \tag{3}$$

The physical interpretation of U_i is the interfacial transmission matrix of heat from layer $(i+1)$ to i, and consists of the items with the form of

$$(1\pm k_{i+1}\sigma_{i+1}/k_i\sigma_i\mp k_{i+1}\sigma_{i+1}R_{i,i+1})\times\exp[\mp\sigma_{i+1}(h_{i+1}-h_i)], \tag{4}$$

where $R_{i,i+1}$ is the thermal contact resistance between layer i and $(i+1)$. Details of the parameters can be found in Ref. 18.

The phase shift between the thermal radiation of the sample surface and the modulated laser beam can be extracted from the above solution. Then trial values of unknown properties, such as thermal conductivity, thermal diffusivity, and thermal contact resistances in Eq. (4), are used to calculate the theoretical values of phase shift at each experimental frequency. For each trial value, the sum of the square of the difference between calculated values and experimental ones is calculated. The trial values giving the best fit of the experimental data are taken as the material properties.

III. RESULTS AND DISCUSSION

A. System calibration

We are interested in measuring the phase shift (time delay) between the thermal radiation and the modulated laser beam, but the measurement will inevitably include a time delay induced by the system. This time delay is calibrated by measuring the reflected laser beam from the sample.[17] Figure 4 presents the measured phase shift for the reflected laser beam. Without instrument time delay, this phase shift would be 0°. From the measured phase shift, the absolute time delay induced by the system is calculated as $(0-f_{\text{cal}})/360/f$, where f_{cal} and f are the calibration phase shift and modula-

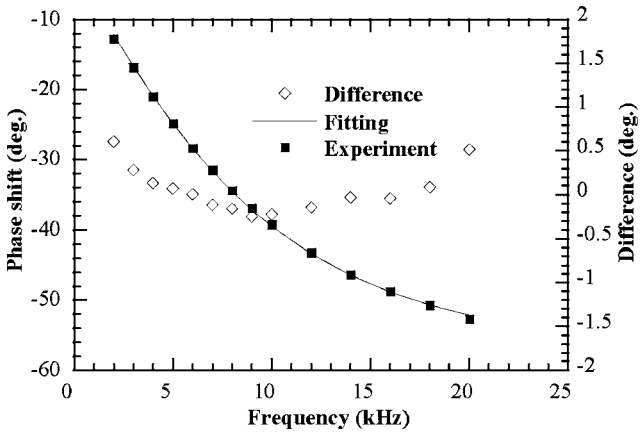

FIG. 5. Data fitting of phase shift for the thermal radiation from the PMMA sample surface.

tion frequency, respectively. In Fig. 4, it is evident that the time delay induced by the system is about 500–800 ns.

B. Measurement results of PMMA and hybrid films

The thermophysical properties of pure PMMA films are measured first. The experimental setup is calibrated before each measurement. Then the phase shift of the thermal radiation is measured in a frequency range of 2–20 kHz. The real phase shift of the thermal radiation is $\phi_{\mathrm{mea}}-\phi_{\mathrm{cal}}$, where ϕ_{mea} is the raw data of the measured phase shift for thermal radiation. Figure 5 shows the absolute phase shift of the thermal radiation signal from the Cr surface, as well as the fitting results. For experimental result fitting, the physical model developed by Xu and co-workers[9,18] is used. During the phase shift fitting, the thermal conductivity and density are given different trial values to get the best fit of the experimental data. The sample consists of different layers, including the air at the top of the Cr film, the Cr film, the PMMA film, Si substrate (437 μm thick), and the air below the Si substrate. Volumetric absorption of the laser beam in the Cr coating is considered, and the optical penetration depth of bulk Cr is 14.6 nm.[19] The thermal contact resistance at the Cr/PMMA and PMMA/Si interfaces is also considered.

Figure 5 shows that the fitting result and the experimental data agree well each other. The differences between them are also plotted. It is observed that most of the differences are around or less than 0.2°, which is consistent with the measurement uncertainty observed in our experiment. Based on phase shift fitting, the measured effective thermal conductivity (k_{eff}) of the PMMA film is determined to be 0.149 W/m K. Compared with the thermal conductivity of bulk PMMA, the measured value of PMMA thin film is smaller. The measured effective volumetric specific heat $(\rho c_p)_{\mathrm{eff}}$ is calculated as 1086 kJ/m^3 K, which is much smaller than that of bulk PMMA, 1614.1 kJ/m^3 K at 298.15 K.[4] Based on data fitting, we also determine the thermal contact resistances at the Cr/PMMA and PMMA/Si interfaces are less than 1×10^{-8} K m^2/W. Considering the coating method of PMMA and Cr films, the small contact resistance is reasonable.

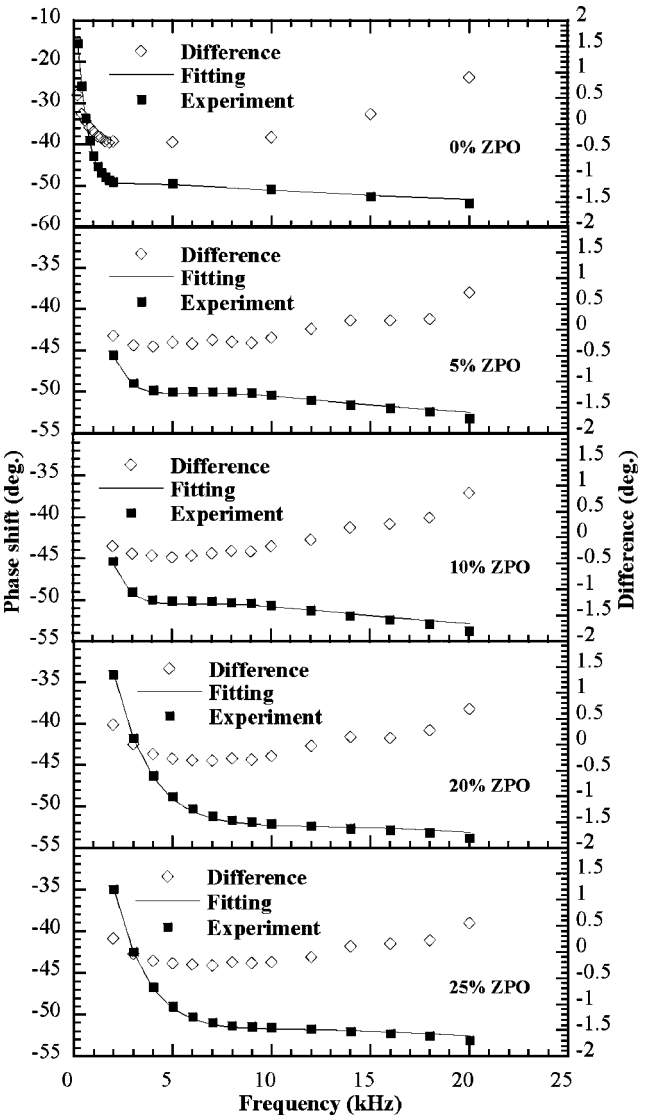

FIG. 6. Data fitting of phase shift for the thermal radiation from the hybrid sample surfaces.

The thermal properties of samples with ZPO molar concentration [ZPO/(MAPTMS+ZPO)] of 0%, 5%, 10%, 20%, and 25% are measured. The 0% molar concentration of ZPO means the hybrid film is composed of only SiO_2 network and PMMA network. Figure 6 shows that the fitting result and the experimental data agree well each other and the differences between them are less than 1°. The measured effective thermal properties are listed in Table I. It shows that the effect of the concentration of ZPO on the thermal properties is not obvious. For the hybrid films, the thermal properties can be affected by the structure, such as porosity, nonuniform thickness, and nonuniform compositions, as well as the material concentration. Table I shows that the measured volumetric specific heat values of hybrid films and PMMA films are much smaller than the value of bulk PMMA, and the porosity or nonuniformity of films needs to be considered in interpreting the data.

In order to evaluate the uncertainty of the measurement, the samples are measured twice and the results are shown in Table I. For hybrid films, most of the variations of thermal

TABLE I. Measured and effective physical properties of hybrid films and PMMA film.

Molar concentration ZPO/(MAPTMS+ZPO)	0%	5%	10%	20%	25%	PMMA
Thickness (μm)	8.3	6.6	6.3	4.1	4.4	2.15
k_{eff}(W/m K) [a]	0.138	0.158	0.144	0.131	0.148	0.149
k_{eff}(W/m K) [b]	···	0.162	0.155	0.139	0.147	0.143
k_{eff}(W/m K) [c]	···	0.143	0.143	0.138	0.139	0.133
$\rho \cdot c_p$(10^6 J/m^3 K) [a]	1.030	1.115	1.087	1.119	1.169	1.086
$\rho \cdot c_p$(10^6 J/m^3 K) [b]	···	1.179	1.140	1.120	1.178	0.946
$\rho \cdot c_p$(10^6 J/m^3 K) [c]	···	1.119	1.143	1.190	1.084	1.014
φ(%) [d]	35.3	29.0	32.1	31.2	28.6	32.7
k_{bulk}(W/m K) [d]	0.251	0.255	0.246	0.220	0.237	0.258

[a]Measurement results for the first time.
[b]Measurement results for the second time.
[c]Measurement results of unheated samples.
[d]Calculated using the measurement result of the first time.

conductivity and volumetric specific heat are all less than 5%, and for PMMA films the variations are about 10%. This indicates sound repeatability of the measurement. The high variations for PMMA films maybe related with the nonuniformity of structure, such as thickness and cavities.

C. Volume fraction of cavities and its effect on thermal conductivity

The effect of moisture on the material and surface is evaluated first. Another group of samples with the same ZPO concentration without preheating are measured and the results are listed in Table I. Compared with the measurement results for preheated samples, most of the variations of thermal conductivity and volumetric specific heat are less than 6%. Considering the measurement uncertainty (5% for hybrid films), the effect of moisture is negligible. The effect of nonuniformity of films is studied as well in this work. The sample with the ZPO molar concentration of 25% is measured at four different points. These four points are located at the four corners of the sample. The results in Table II show that the variations of thermal conductivity and volumetric specific heat are found to be less than 9% for these four points. Considering the measurement uncertainty, the film has uniform property from location to location, and the data reported in Table I represent the typical properties of the film.

In order to rule out the effect of the cavities on the thermal conductivity reduction, the effective medium theory and Maxwell's method[20] are applied to calculate the bulk thermal conductivity of the hybrid film. The Maxwell equation considering the effect of cavities on the overall thermal conductivity is expressed as

TABLE II. Measurement results at four different spots of sample with 25% ZPO.

Measurement point	1	2	3	4
Thickness (μm)	4.4	4.4	4.4	4.4
k_{eff}(W/m K)	0.139	0.130	0.128	0.137
$\rho \cdot c_p$(10^6 J/m^3 K)	1.063	1.098	1.030	1.084

$$\frac{k_{\text{eff}}}{k_{\text{bulk}}} = 1 + \frac{3(\gamma - 1)\varphi}{(\gamma + 2) - (\gamma - 1)\varphi}, \tag{5}$$

where γ is the ratio of thermal conductivity of cavities to that of the hybrid film (γ=0 in this work), φ is the volume fraction of cavities, k_{eff} is the measured effective thermal conductivity, and k_{bulk} is the thermal conductivity for bulk hybrid film without cavities. The volume fraction can be calculated as

$$\varphi = 1 - \frac{(\rho c_p)_{\text{eff}}}{(\rho c_p)_{\text{bulk}}}, \tag{6}$$

where $(\rho c_p)_{\text{eff}}$ and $(\rho c_p)_{\text{bulk}}$ are the measured effective volumetric specific heat and volumetric specific heat of bulk hybrid films, respectively. For a compound system with n types of materials, the effective volumetric specific heat can be predicted as

$$(\rho c_p)_{\text{bulk}} = \sum_{i}^{n} \phi_i \rho_i c_{p,i}, \tag{7}$$

where ϕ_i is the volume fraction of material i. For Eq. (7), the hybrid films are simply treated as the composite with PMMA, SiO_2, and ZrO_2, and their volume fractions are obtained using molar concentration. The details of parameters used in Eq. (7) are listed in Table III. Finally, the volume fraction of cavities and the effective thermal conductivity of bulk hybrid films without cavities are predicted and listed in Table I.

The volume fractions of cavities in hybrid films are predicted to be varied from 28.6% to 35.3%. There are several mechanisms for the formation of cavities in the hybrid films. It is well known that the sol-gel method offers the advantages of tailor-made porosity which may control the analyte diffusion, leachability, and refractive index of hybrid organic-inorganic material.[21] A porous gel will first be formed during the polycondensation of the hydroxylated units,[22] and then the network will be densified by heat treatment. Considering the fact that the thicknesses of the hybrid films are in the order of micrometers, the size of cavities formed after densification should be at the scale of nanometers. Previous research also showed that the molecular cage-

TABLE III. Volume fraction of components and the resulted volumetric specific heat in Eq. (7).

Molar concentration ZPO/(MAPTMS+ZPO)	0%	5%	10%	20%	25%	PMMA
PMMA (vol %)	86.65	66.01	79.00	78.86	78.77	100.00
SiO_2 (vol %)	13.35	32.63	19.30	17.65	16.80	0.00
ZrO_2 (vol %)	0.00	1.36	1.70	3.49	4.43	0.00
$(\rho \cdot c_p)_{\text{bulk}}(10^6\ \text{J/m}^3\ \text{K})$	1589.9	1571.1	1599.9	1625.1	1638.3	1614.1

like pores at atomic levels or pores of nanometer size can form during the doping of amorphous silica when the chemical bonds are opened up.[23] The inorganic part of zirconia network and silica network in our hybrid material are amorphous. The molecular or nanopores can be formed inside the network during the process of hydrolyzation of inorganic part. Moreover, considering the inorganic network (Zr–O–Zr and Si–O–Si) has excellent mechanical stability, the densification process through heat treatment will have less effect on the molecular or nanocavities inside the network.

The scanning electron microscopy (SEM) pictures in Fig. 7 are the cross section of hybrid film with 10% ZPO, which confirm the idea about cavities. The pores inside the hybrid film, which is the layer above the dashed line, are in the order of micrometer or submicrometer. Another obvious characteristic is that there are plenty of micrometer pores on the surface of hybrid film, which may introduce great uncertainty in the determination of film thickness. From Table I, we find that the predicted thermal conductivity of bulk PMMA is a little bigger than that of the literature value, 0.21 W/m K.[24] One of the reasons for this deviation is Eq. (5) used for predicting the bulk thermal conductivity. Equation (5) is more accurate for systems with a lower concentration of cavities. Moreover, judging from Fig. 7, the predicted volume fraction of cavities for hybrid films may be overestimated. There are some factors which can introduce uncertainties to the prediction of φ when using the effective medium theory, such as the estimation of the bulk volumetric specific heat. Equation (7) is reasonable and accurate for simple compound systems. This equation is not strictly valid for the highly disordered materials including hybrid polymers in which different molecules are connected by chemical bonds. At the same time, the uncertainty of φ can be introduced by the measured $(\rho c_p)_{\text{eff}}$ from Eq. (6). In fact, for the physical model employed in this work, there are two parameters that can be obtained accurately; one is $k\rho c_p$ and the other one is L/k, which will be explained in the next section. The uncertainty in volumetric specific heat can be introduced by the measured uncertainty of film thickness. Figure 7 shows that the thickness has the nonuniformity of 1–2 μm, which will bring great uncertainties into the thermal conductivity and volumetric specific heat. The volume fraction of the cavities reported in Table I includes the effect of the large pores in the surface observed in Fig. 7. Figure 8 is the optical microscope picture of the hybrid film with 10% ZPO, which confirms the film surface is nonuniform at large scale. We can re-evaluate the volume fraction of cavities of PMMA using Eq. (5) directly and the below equation,

$$(k\rho c_p)_{\text{eff}} = (k\rho c_p)_{\text{bulk}}(1-\varphi)(1-3\varphi/(2+\varphi)), \tag{8}$$

because the thermal conductivity or $k\rho c_p$ of bulk PMMA can be determined from the literature value. The re-estimated volume fraction from Eqs. (5) and (8) is 21.4% and 26.5%, respectively. For the PMMA film, the volumetric specific heat of bulk material can be found in literatures. The large discrepancy of estimated results of volume fraction of cavities using Eqs. (5), (6), and (8) show that the error of volume fraction of cavities should mainly come from the uncertainty of thickness. Additionally, the thickness of PMMA is obviously smaller than that of hybrid films and comparable to the thickness uncertainty. This explains why the measurement

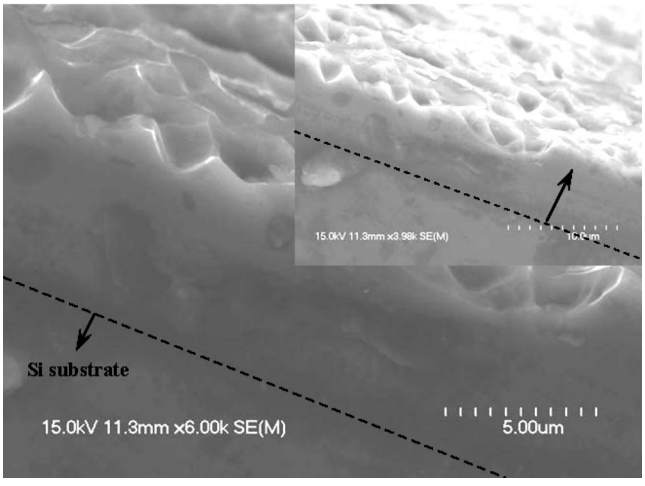

FIG. 7. SEM pictures of the hybrid film with 10% ZPO (6.3 μm thick).

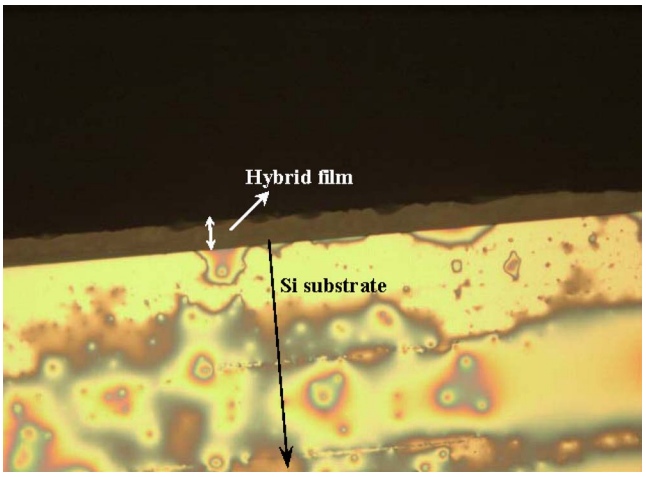

FIG. 8. (Color online) Optical microscope picture of the hybrid film with 10% ZPO (6.3 μm thick).

repeatability for PMMA is not as good as that of hybrid films.

D. The effect of ZPO concentration on the effective thermal properties

Table I shows the thermal conductivity of hybrid films is smaller than that of PMMA. The resulting hybrid material can be pictured as an inorganic backbone (Si–O–Si bonds) with homogeneously dispersed zirconium-rich clusters and organic network (PMMA).[25] The amorphous inorganic material doped in PMMA might decrease the phonon mean free path and cutoff its spectrum. Actually the mean free path of amorphous SiO_2 was calculated to be smaller than that of PMMA.[6] Through asymmetric stretching vibration of Si–O–Si bridging sequences, the inorganic network can change the vibration spectra of the hybrid material.[22] This might introduce extra scattering to the phonons in PMMA and make the thermal conductivity smaller. At the same time, the size of molecular and nanocavities are comparable to or larger than the mean free path of phonons (which is on the level of a few angstrom), which can strongly enhance the phonon scattering. Consequently, the thermal conductivity of hybrid films is expected to decrease according to the following relationship:[6] $k=(\frac{1}{3})Cv\bar{l}$, where C, v, and $\bar{l}$ are the specific heat (per unit volume), phonon velocity, and mean free path, respectively. In Table I, we also find that the ZPO concentration has some insignificant effect on the thermal conductivity of hybrid films. The predicted bulk thermal conductivity without cavities is about 0.220–0.251 W/m K. The difference among hybrid films is the concentration of zirconia clusters, which may exist as the form of nanoparticles.[25] Based on the molar concentration, the volume fraction of zirconia clusters are calculated to be less than 5% for all the films. The thermal conductivity of zirconia nanoclusters is comparable to that of PMMA since they are amorphous and at nanoscales or smaller. Estimated from Eq. (5), we know that if γ takes 2.5, the thermal conductivity change introduced by the zirconia clusters will not exceed 5%, which is comparable to the measurement uncertainty. It is conclusive that the thermal conductivity of hybrid films is dominated by the PMMA and SiO_2 networks. PMMA hybrid films are important materials in applications in integrated optics, and the ZPO is mixed with MAA to produce ZrO_2, which is used to adjust the refractive index of the product. Our measurement concludes that the addition of ZPO adjusts the optic property of film without changing its thermal conductivity significantly. This will provide valuable guidance on the thermal management during device packaging.

In the measurement, the thermal conductivity and thermal diffusivity are very sensitive to the volumetric specific heat and thickness. From the physical model described by Eq. (4), it is observed that for a given multilayer sample, the interfacial transmission matrix of heat at every layer (U_i) can be obtained accurately. Then the two parameters $k\sigma$ and σh in Eq. (4) can be determined directly and independently. So during data fitting using trial values of different thermal properties, in fact two properties can be precisely determined: $k\rho c_p$ and L/k. Although the evaluated error of individual thermal parameters during data fitting can be introduced by many factors, the parameters $k\rho c_p$ and L/k can be determined with high accuracy and will not be affected by the uncertainty of thickness measurement. $k\rho c_p$ and L/k are the thermal effusivity and thermal resistance per unit area for the film, respectively. The quantity of thermal effusivity implies dullness or sharpness of the surface temperature change when the heat flux across the surface is changed abruptly. Figure 9 shows the effect of ZPO concentration on the thermal effusivity of hybrid films. The relationship between the measured effective thermal effusivity of hybrid films and that of PMMA is not clear because of the difference in cavities. The hybrid and PMMA films have close thermal effusivities. These results indicate that the rate of the surface temperature change of hybrid films will be similar to that of PMMA films when the heat flux across the surface is changed abruptly. This temperature changing rate will be almost independent of the ZPO concentration. The ZPO addition reduces the thermal effusivity of bulk hybrid films [which is $k_{\text{bulk}}(\rho c_p)_{\text{bulk}}$] without cavities, which are obviously smaller than that of PMMA.

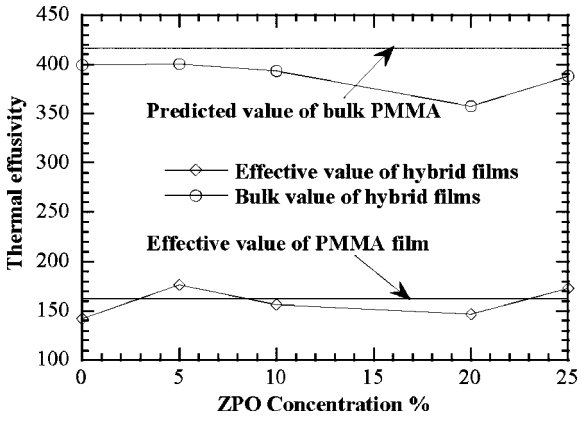

FIG. 9. Effective thermal effusivity and predicted thermal effusivity of bulk PMMA and hybrid films.

IV. CONCLUSIONS

In this work, a photothermal technique was designed to characterize the thermophysical properties of optic films with organic/inorganic hybrid structure. The volume fraction of cavities and its effect on the thermophysical properties were evaluated based on the measured volumetric specific heat. The effective thermal conductivity and thermal effusivity of hybrid films were close to those of PMMA films and did not show strong effect of the ZPO concentration. The large fraction of cavities (confirmed by optical microscopy and SEM pictures) had significant contributions to the reduced thermal conductivity and thermal effusivity. The extracted bulk thermal conductivity and thermal effusivity of the hybrid films showed that addition of ZPO reduced these properties and made them smaller than those of bulk PMMA. Our thermal effusivity study concluded that the response of the surface temperature change to an abrupt heat flux across the surface of hybrid films will be similar to that of PMMA film. The dose of ZPO can adjust the optic property of films without changing their thermophysical properties significantly.

ACKNOWLEDGMENT

This work was supported by National Science Foundation (CMS: 0457471), Nebraska Research Initiative, Air Force Office for Scientific Research, and MURI from ONR. The authors especially appreciate the strong support from the China Scholarship Council for the State Scholarship Fund to pursue the research.

[1]X. Wang, L. Xu, D. Li, L. Liu, and W. Wang, J. Appl. Phys. **94**, 4228 (2003).
[2]D. Li, Y. Zhang, L. Liu, and L. Xu, Opt. Express **14**, 6029 (2006).
[3]S. Rudtsch and U. Hammerschmidt, Int. J. Thermophys. **25**, 1475 (2004).
[4]M. J. Assael, S. Botsios, K. Gialou, and I. N. Metaxa, Int. J. Thermophys. **26**, 1595 (2005).
[5]S. A. Putnam, D. G. Cahill, B. J. Ash, and L. S. Schadler, J. Appl. Phys. **94**, 6785 (2003).
[6]D. G. Cahill and R. O. Pohl, Phys. Rev. B **35**, 4067 (1987).
[7]D. Chu, M. Touzelbaev, K. E. Goodson, S. Babin, and R. F. Pease, J. Vac. Sci. Technol. B **19**, 2874 (2001).
[8]S. Govorkov, W. Ruderman, M. W. Horn, R. B. Goodman, and M. Rothschild, Rev. Sci. Instrum. **68**, 3828 (1997).
[9]X. Wang, H. Hu, and X. Xu ASME J. Heat Transfer **123**, 138 (2001).
[10]D. G. Cahill, Rev. Sci. Instrum. **61**, 802 (1990).
[11]D. G. Cahill and T. H. Allen, Appl. Phys. Lett. **65**, 309 (1994).
[12]M. Okuda and S. Ohkubo, Thin Solid Films **213**, 176 (1992).
[13]K. E. Goodson, M. I. Flik, L. T. Su, and D. A. Antoniadis ASME J. Heat Transfer **116**, 317 (1994).
[14]K. E. Goodson, O. W. Kading, M. Rosler, and R. Zachai, J. Appl. Phys. **77**, 1385 (1995).
[15]Z. L. Wu, M. Reichling, X. Q. Hu, K. Balasubramanian, and K. H. Guenther, Appl. Opt. **32**, 5660 (1993).
[16]H. Machlab, W. A. McGahan, and J. A. Woollam, Thin Solid Films **215**, 103 (1992).
[17]X. Wang, Z. Zhong, and J. Xu, J. Appl. Phys. **97**, 064302 (2005).
[18]H. Hu, X. Wang, and X. Xu, J. Appl. Phys. **86**, 3953 (1999).
[19]J. H. Weaver and H. P. R. Frederikse, *CRC Handbook of Chemistry and Physics*, 74th ed. (CRC, Boca Raton, FL, 1993), pp. 12-109–12-131.
[20]J. C. Maxwell, *Electricity and Magnetism* (Clarendon, Oxford, UK, 1873).
[21]C. Sanchez, B. Lebeau, F. Chaput, and J. P. Boilot, Adv. Mater. (Weinheim, Ger.) **15**, 1969 (2003).
[22]L. Yang, S. S. Saavedra, N. R. Armstrong, and J. Hayes, Anal. Chem. **66**, 1254 (1994).
[23]D. G. Cahill, W. K. Ford, K. E. Goodson, G. D. Mahan, A. Majumdar, H. J. Maris, R. Merlin, and S. R. Phillpot, J. Appl. Phys. **93**, 793 (2003).
[24]J. E. Mark, *Physical Properties of Polymer Handbook* (AIP, Woodbury, NY, 1996), pp. 111–118.
[25]S. Pelissier, D. Blanc, M. P. Andrews, S. I. Najafi, A. V. Tishchenko, and O. Parriaux, Appl. Opt. **38**, 6744 (1999).